Fermi National Accelerator Laboratory

FERMILAB-Conf-93/395-E

DØ

Inclusive Single Muon Production in DØ

Arthur K.A. Maciel
For the DØ Collaboration

Fermi National Accelerator Laboratory
P.O. Box 500, Batavia, Illinois 60510

LAFEX, Centro Brasileiro de Pesquisas Fisicas
Rio de Janeiro, Brasil

December 1993

Presented at the *9th Topical Workshop on Proton-Antiproton Collider Physics*, Tsukuba, Japan, October 18-22, 1993

Disclaimer

Inclusive Single Muon Production in DØ

Arthur K. A. Maciel, for the DØ Collaboration

Laboratório de Física Experimental de
Altas Energias e Cosmologia - LAFEX
Centro Brasileiro de Pesquisa Físicas
Rio de Janeiro, Brasil

Preliminary cross section measurements from the DØ experiment at Fermilab for the inclusive production of single muons in proton-antiproton collisions at $\sqrt{s} = 1.8$ TeV are presented. It is found that the experimental results are consistent with those obtained from a Monte Carlo simulation using N.L.O. calculations from ISAJET.

1. Introduction

There are of course several reasons for seeking inclusive muon production spectra in high energy proton-antiproton collisions, and among these reasons, one of particular interest is the study of Heavy Flavour Production. Indeed, prompt muons can be very efficient heavy flavour tags, and therefore from the single muon distributions one can, in a model dependent fashion, unfold heavy quark distributions. These in turn can be used to test perturbative QCD predictions and their dependence on different parton density functions in the proton. Those steps in fact briefly summarize the general goals of the present analysis, which is now at the stage of presenting its preliminary results for single muon production yields.

The components of the DØ detector relevant for this analysis are the central tracking chambers, the uranium-liquid argon calorimeter and the muon detection system. A detailed description of each component can be found in reference [1]. The muon detection system is the outermost subdetector of DØ. It consists of 3 layers of muon chambers (stacks of proportional drift tubes) with solid iron magnetic toroids sandwiched between the innermost two, providing momentum measurement.

In section 2 the various physics processes which contribute muons to the inclusive sample are presented. Section 3 describes the data sample and summarizes the main aspects of its analysis. Results are presented in section 4, followed by a few concluding remarks.

2. Single μ Production

Within the p_T range spanned by the present analysis there are four major physics sources that contribute to the final spectrum. These are: (i) Muons from the in flight decays of pions and kaons within the detector volume. (ii) QCD $b\bar{b}$ production, with (spectator model picture) decays $b \rightarrow \mu X$ and $b \rightarrow c \rightarrow \mu X$. (iii) QCD $c\bar{c}$ production, $c \rightarrow \mu X$. (iv) Drell-Yan production of W$\rightarrow \mu\nu$ and Z$\rightarrow \mu\mu$. Their expected yields, according to a Monte

Carlo simulation using next to leading order (N.L.O.) QCD calculations with ISAJET [2] are represented by the smooth lines in figure 2 , where the solid line shows the summed total contribution.

Each particular physics process dominates the muon spectrum over a certain p_T^μ range. For instance, in the central detector (fig. 2(a)), $|\eta| < 1.0$) these ranges are roughly, $p_T^\mu < 5\ GeV$ for π/K decays, $10 < p_T^\mu < 25\ GeV$ for QCD heavy flavour production, and $p_T^\mu > 30\ GeV$ for W-Z production. At higher rapidities (fig. 2(c)), this last process becomes negligible.

3. Data Analysis

Due to the high trigger rates for single muons, dedicated runs with moderate trigger prescales were taken for the determination of the inclusive muon cross section. Three independent samples, corresponding to three different rapidity regions in the detector, were analysed separately. The total integrated luminosity in each sample is $\int \mathcal{L}\,dt = (80 \pm 9.6)nb^{-1}$ for the central region $|\eta| < 1.0$, $\int \mathcal{L}\,dt = (11 \pm 1.3)nb^{-1}$ for the end caps region $1.0 < |\eta| < 1.6$, and $\int \mathcal{L}\,dt = (6.7 \pm 0.8)nb^{-1}$ for the small angle region $2.2 < |\eta| < 3.3$. The region $1.6 < |\eta| < 2.2$ is currently under active study.

The DØ trigger system consists of two hardware trigger levels (level 0 and level 1), and a software level (level 2). The level 0 trigger uses a scintillator hodoscope to select inelastic collisions which occur within 1 meter of the nominal interaction point along the beam direction. The level 1 muon trigger requires that hits in 60 cm wide roads from the 3 layers of muon chambers be consistent with a track pointing to the interaction region. At level 2 the muon track is reconstructed and is required to pass quality cuts along with a minimum p_T of 3 GeV (2 GeV in the case of the small angle detector).

Single muon events are then reconstructed offline and are retained for further analysis if they contain at least one muon track satisfying the following criteria:

Hits in all 3 layers of muon chambers
Good track quality and consistent vertex association
In time with beam crossing
A minimum of 1 GeV of energy deposited in the calorimeter
A matching track in the central tracking chambers

The muon momentum resolution varies with the momentum itself. In the lower end of the spectrum it is roughly 20% and is limited mainly by multiple Coulomb scattering. The total DØ thickness (calorimeter and iron toroids) varies between 14 and 19 absorption lengths depending on the polar angle θ, and this constitutes a comfortable shielding against hadron punchthrough, which does not exceed 1% of the final muon sample. At the high end of the p_T spectrum, the presently achieved chamber spatial resolution ($\sim 0.5\ mm$) is the main limiting factor, with momentum uncertainties reaching 50% at 60 GeV p_T^μ .

After the offline cuts, there is still some background due to cosmic rays and hit

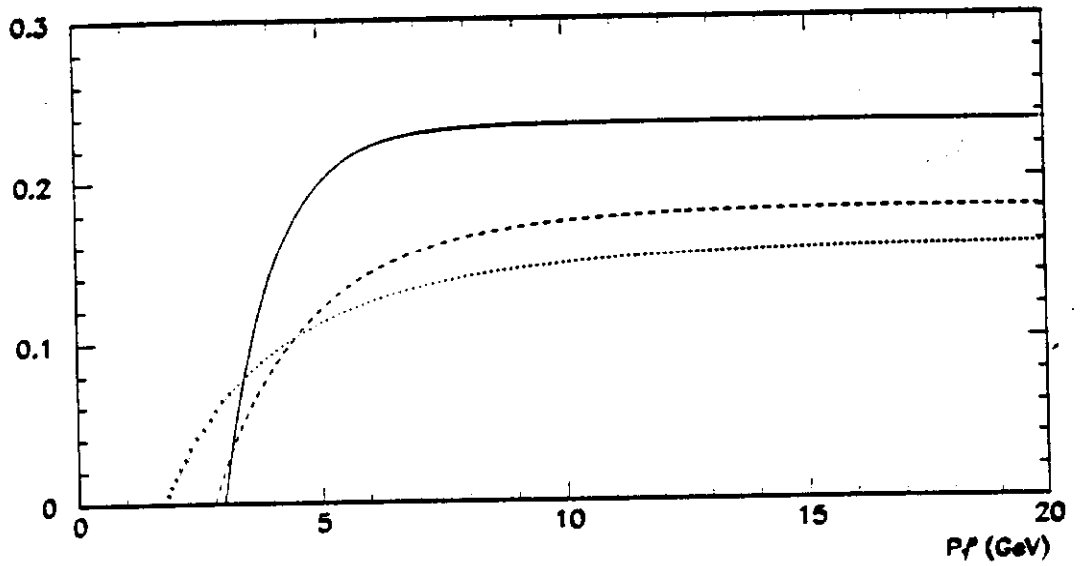

Figure 1: Muon Detection Efficiencies:
solid - Central Detector, dashed - End Caps,
dotted - Forward Detector.

combinatorics. These have been estimated and subtracted in a p_T dependent fashion. The uncertainties in the cross section, associated with the background subtraction procedures, are of the order of 10%.

4. Inclusive μ Cross Section

The detection efficiency for single muons was estimated using a sample of inclusive Monte Carlo $b\bar{b} \rightarrow \mu X$ and $c\bar{c} \rightarrow \mu X$ events, and also the real data wherever possible for cross checks. The Monte Carlo sample includes full detector and trigger simulation, and was passed through the same analysis routines as used for the real data. In a few cases, where detector effects are not precisely modeled by the simulation programs, real data were used to estimate the corrections.

The overall detection efficiencies as a function of p_T^μ are shown in Figure 1 for each of the rapidity regions independently analyzed: Central (solid line), End Caps (dashed line) and Forward (dotted line) detectors. The systematic uncertainties on the determination of efficiencies were estimated to be of the order of 20%. There are plans to reduce that value in the near future with the use of a large cosmic ray data set.

The normalized data, corrected for the efficiency and plotted in variable p_T^μ bin sizes that conform to the muon momentum resolution of the detector, are shown in Figs. 2(a)

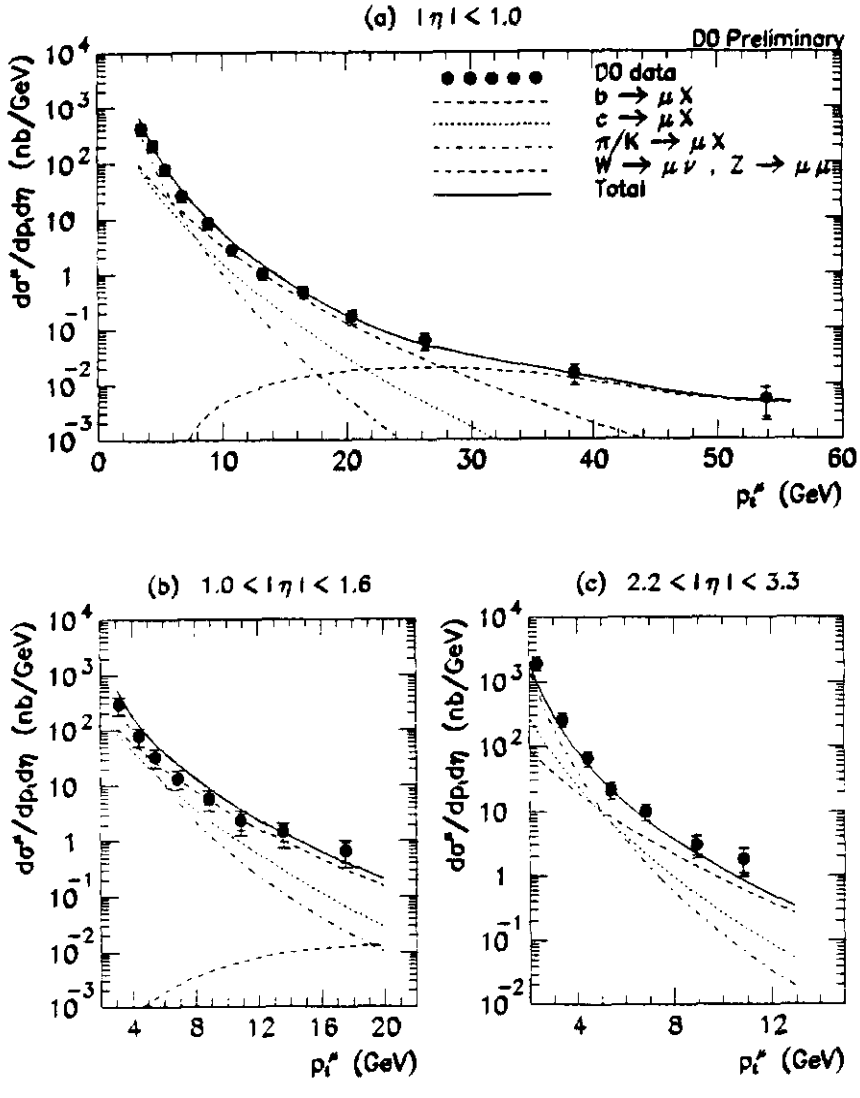

Figure 2: Single Muon Inclusive Cross Sections. (a) Central Detector, (b) End Caps, (c) Forward Detector.

for $|\eta| < 1.0$, $2(b)$ for $1.0 < |\eta| < 1.6$ and $2(c)$ for $2.2 < |\eta| < 3.3$. The dashed, dotted, dot-dashed, and solid lines represent the different contributions to the single muon spectrum expected from b, c and π/K decays, and the sum of all the contributions respectively, as described in section 2.

A comparison between the data points and the summed Monte Carlo distributions shows fairly good agreement both in shape and absolute value within the total experimental uncertainties which are of the order of 30% . The smaller error bars on the data points represent the statistical uncertainties, while the full bars are for the statistical and systematic errors added in quadrature. The main sources of systematic errors are the luminosity measurement, efficiency estimates and background subtraction.

The most direct evidence for the different physics sources that contribute muons to the final sample comes from the muon and jet association characteristics. Despite the absence of any jet requirement in the analysis, about 65% of all muons have a neighbouring jet (within a cone of 0.7) with transverse energy E_T above 10 GeV, and this jet has either the first or second largest E_T in the event. This is the typical signature for semileptonic decays, and the transverse momentum of the muon with respect to its neighbouring jet (p_T^{rel}) increases with the Q-value of the decay. This variable thus provides a consistency check of the relative amounts of $b\bar{b}/c\bar{c}$ as a function of p_T^{μ} as asserted in Figure 2. This check will be quantified in the near future.

The separation of the $b\bar{b}$ muons from the inclusive sample is still work in progress but, as an example, Figure 3 shows the p_T^{rel} distributions of the non isolated muons in the final spectrum for $p_T^{\mu} < 9\ GeV$ (left), $p_T^{\mu} > 9\ GeV$ (right), Data (top) and M.Carlo (bottom). The Monte Carlo sample is the same as that used for the cross section predictions in Figure 2. A significant difference in p_T^{rel} is evident between the low and high p_T^{μ} data subsamples, a feature also present in the Monte Carlo counterparts, despite the poor statistics at high p_T.

5. Conclusions

The DØ detector has demonstrated a good ability to measure muons, with very low punchthrough, good cosmic rejection and efficient heavy flavour tagging. Preliminary measurements of the inclusive single muon cross section show good agreement with theoretical expectations in three different physics regimes, over a wide range of p_T and rapidity. The low p_T spectrum is dominated by pion and kaon decays, continues smoothly into the QCD heavy flavour production region, and further extends to the higher p_T region where weak W production and decay is the predominant muon source. From jet association characteristics we have good evidence of the different content of the muon sources in these various p_T ranges.

The measurements will be extended to cover all rapidities (up to 3.3) with reduced systematic uncertainties and higher statistics as more data is added to the analysis during the upcoming Run 1b at the Fermilab Collider. Work currently in progress includes the separation of the $b\bar{b}$ component from the inclusive muon sample for the extraction of the b production cross section.

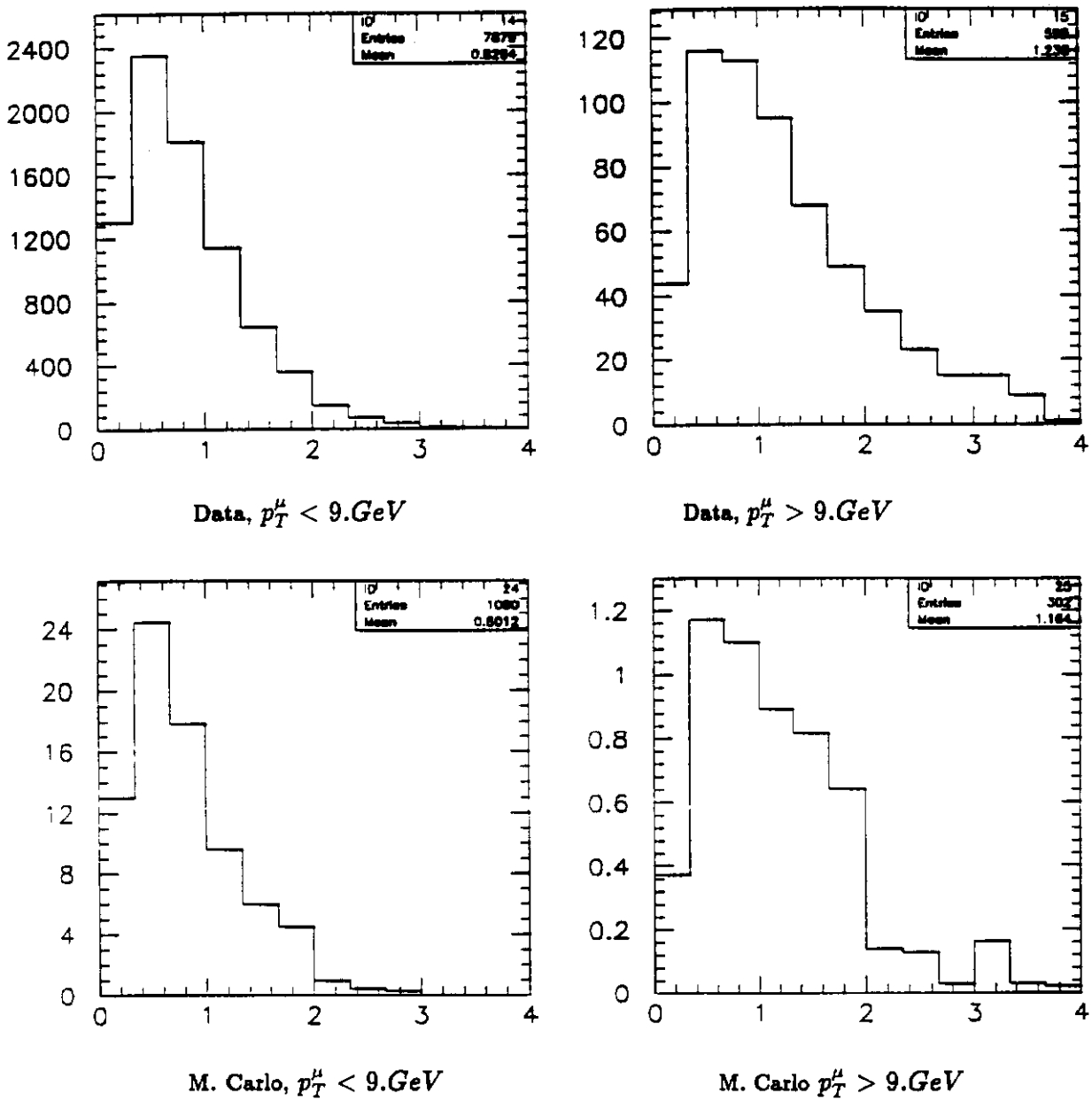

Data, $p_T^\mu < 9.GeV$

Data, $p_T^\mu > 9.GeV$

M. Carlo, $p_T^\mu < 9.GeV$

M. Carlo $p_T^\mu > 9.GeV$

Figure 3: Distribution (arbitrary units) of muon transverse momentum with respect to neighbouring jet axis (p_T^{rel}, in GeV) for Data and M. Carlo, in two different ranges of p_T^μ.

The author gratefully acknowledges the support received from AIAFEX (Rio de Janeiro) and from the University of Tsukuba, which rendered possible his participation in the Workshop.

6. References

1. S. Abachi *et al.*, "The DØ Detector", submitted to NIM.
2. F. Paige and S.D. Protopopescu, *BNL* 38034 (1986).